Egyptian Geophysical Society
EGS Journal, Vol. 21, No. 1, 11-19 (2023)

APPLICATION OF GROUND PENETRATING RADAR (GPR) TECHNIQUE TO DETECT POSSIBLE HIDDEN GAPS OR VOIDS IN AN AGRICULTURAL LAND, NAG HAMMADI, QENA, EGYPT

S.B.A. YOUSSEF, M.A. SHAHEEN and M.H.M. YOUSEF

Nuclear Materials Authority, Cairo, Egypt

تطبيق تقنية الرادار للكشف عن الفجوات المخفية المحتملة فى أرض زراعية ، نجع حمادى ، قنا ، مصر

الخلاصة: منطقة الدراسة المختارة هي أرض زراعية تبلغ مساحتها حوالى 600 متر . مربع الهدف الرئيسي من هذه الدراسة هو الكشف عن حجم وعمق الفراغ أو الفجوات الجوفية (المجارى) لمعالجة فقدان مياه الري. تم إجراء ستة عشر ا مقطعا جانبيا باستخدام تقنية الرادار بأطوال مختلفة تتراوح من 32 الى 35 مترا ، مع مسافة فاصلة بني اخلطوط تبلغ 1 متر . يشمل التعامل مع هذه البيانات تفسير خطوط المسح الرادارى للكشف عن مواقع الفراغات والكهوف فى المنطقة المختارة ، وتحديد طرق التعامل مع هذه المواقع لتقليل الفاقد من مياه الري. توضح هذه الدراسة مواقع تباينات الالوان المختلفة والانعكاسات العالية واتساع الاشارات المنعكسة ، مقارنة بالتربة المحيطه ؛ كما أن تشتت الاشارات أعلى من الطبقة الحاوية فى هذه المواقع مما قد يكشف عن الفراغات والكهوف المحتملة فى منطقة الدراسة. تتراوح أعماق الاهداف المحتملة من 7.0متر الى 8.0 متر . تم إجراء تحليل ثلاثى الابعاد لمجموع ملفات تعريف GPR لتأكيد وجود الهدف المخفى المحتمل والاعماق الدقيقة لهذه المواقع. تم عمل أربع شرائح زمنية مختلفة (وقت الإختراق فى اتجاهين) ، كما تم عمل مقطعين فى الاتجاه السينى والصادى لإظهار الهدف المخفي المحتمل . تتوافق النتائج مع العمق الذي تم الحصول عليه من الصورة ثنائية الابعاد.

ABSTRACT: *The selected area is an agricultural land of approximately 600 m square. The main target of this study is to detect the size and depth of the subsurface voids or gaps (sinkholes) to treat the problem of irrigation water loss. Sixteen GPR profiles of different lengths were conducted ranging from 32-35 m, with a separation of 1 m width. The interpretation of GPR profiles reveals the locations of the voids in the selected area, and determine the effective ways to deal with these defects. Results showed locations of different color contrasts and high reflections amplitude of the reflected signals, compared to the surrounding soil; also the higher scattering compare to the bed layer in these locations reveals possible voids in the study area. The depths of the possible targets range from 7.0 m to 8.0 m. 3D analysis was performed for the total GPR profiles to confirm the presence of the possible hidden target and the accurate depths of these objects. Four time-slicing at different (two-way travel time) TWTT were selected together with two X-cut and two Y-cut were done to track the possible hidden target. These results were in agreement with the results obtained from the 2D image. Such information reveal the important of Radar technique in handing the geotechnical problems.*

1. INTRODUCTION

The area of the present study is located in the Nag Hammadi city, Qena governorate (Fig. 1). Where a piece l of an agricultural land of approximately an area of 600 m square was selected. During the irrigating of this agricultural land, water seeps into the ground. The downward movement of water may also transport soils, resulting in fertilizing ground loss and surface depressions called "sinkholes", a GPR survey was conducted to determine these subsurface features and the possible occurrence of voids (sinkholes) responsible for the irrigation water loos. The sedimentary succession in the study area belongs to the Nile valley succession of the late Cretaceous to early Eocene, a dry mud and sandy mud overlying the wet sand layer (Said, 1981). Ground-penetrating radar is selected to help identifying the locations of sinkholes in the selected area to determine then options ways to deal with the loss of the irrigation water.

The effectiveness of a geophysical survey is typically conditioned by the existence of contrast between the measured physical properties among the study area. Therefore, considering changes in physical properties of material due to dissolution, erosion, and/or subsidence involved in the development of sinkholes, geophysical methods are excellent tools for indirect investigation (Hoover 2003). In general, the use of geophysical surveys in the characterization of karst terrains consists of the detection and mapping of the extension of sinkholes as well as information about the depth of the water table, direction of the underground flow, and depth of the karst rocks (Chalikakis et al. 2011).

Despite the countless geophysical investigations carried out on karst terrains worldwide, (mainly for mapping cavities) GPR method has proven to be the most efficient geophysical method for identifying geometric karst features. At the past couple of decades the use of the GPR method has increased and many improvements have been successfully implemented (McMechan et al. 1998; Zisman et al. 2005; Kruse et al. 2006; Rodriguez et al. 2014; Sevil et al. 2017; Hussain et al. 2020).

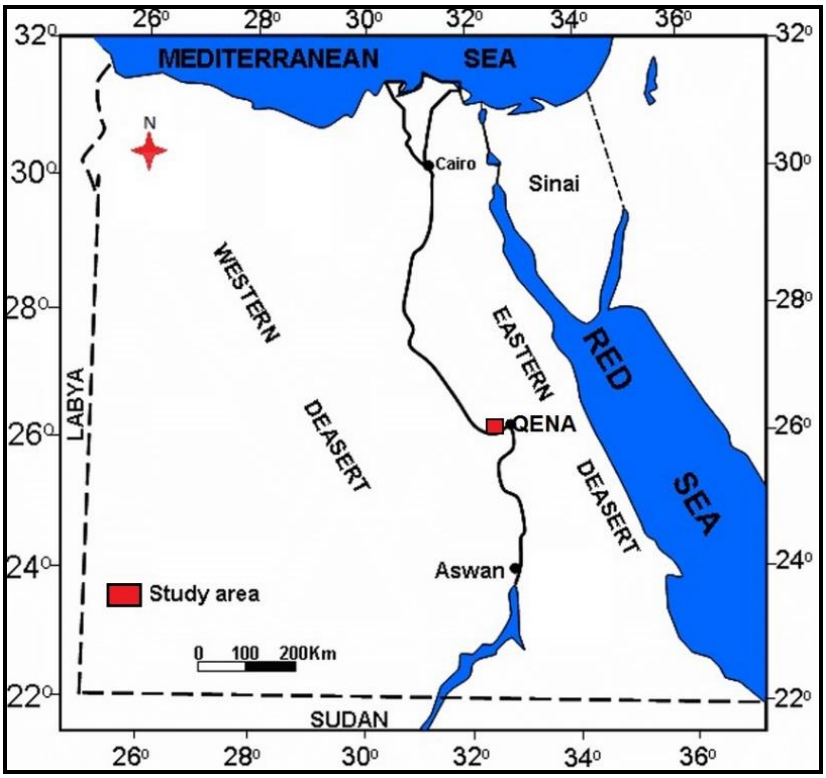

Fig. (1): A location map of the study area.

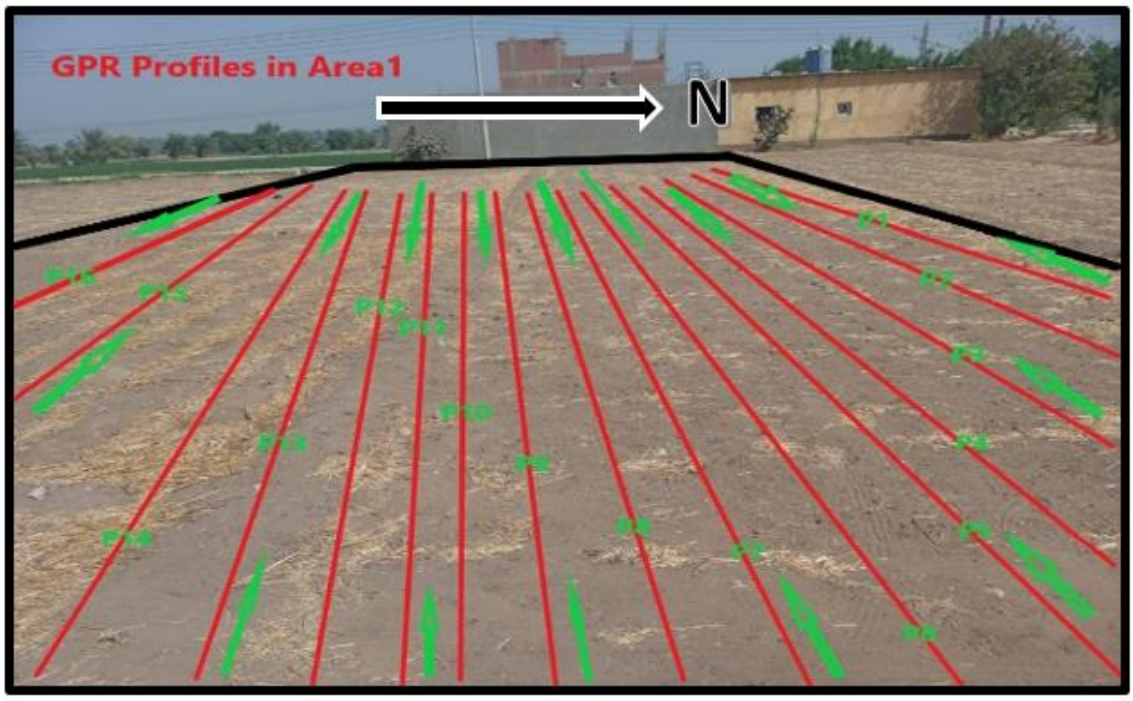

Fig. (2): Location of GPR profiles in the study area.

2. Ground Penetrating Radar (GPR) Survey

2.1. GPR basic concept

The physical principle and data acquisition of GPR methodology are similar to the seismic reflection and the sonar techniques, except for the fact that the GPR is based on the reflection of electromagnetic waves (Casas et al. 2000). According to Annan (2002), this method stands out for shallow investigations, due to its high resolution and the acquisition of a large volume of data in a short period of time. The depth of investigation is a limitation of the GPR method, and is influenced by many factors including geometric scattering, attenuation by the terrain, and partition of energy at the interfaces,

which are all related to the loss of energy during the propagation of the electromagnetic wave (Bradford 2007). The depth of investigation and resolution of GPR vary according to the frequency of the antenna. The higher the frequency, the higher the vertical resolution and the lower the depth of investigation, and vice versa.

A ground-penetrating radar instrument includes a transmitter, a receiver, and a data collection device. The transmitter sends radio pulses from an antenna into the ground. A receiver picks up reflections received from this radio signal, the strength and direction of the reflected signal give the size and depth of the reflecting object (Daniels, 1996). The advantage of GPR is that it records detailed vertical soil profiles rather than just generating horizontal plan maps. It must be remembered that GPR doesn't only image targets in the subsurface, it provides a 2D record of the 3D waves bouncing of objects on the ground (Davis et al., 1989). Linear features which are aligned with the GPR's electrical field will not produce high reflectance values. However, this means that GPR is good at distinguishing linear features if only run perpendicular to the path of the antenna (Sharma, 1997).

2.2. GPR instrument

In the present study, a Sweden MALA GPR system was used with a 100 MHz antennae (Fig. 3). It provides a detailed look at what's beneath the surface. The system offers leading-edge GPR technology, with full digital control to all setup parameters and a multi-channel color display.

2.3. Data collection and processing

Sixteen GPR profiles of E-W direction were conducted of different lengths ranging from 32-35 m, with a line separation of 1 m width.. The objective of this study is to detect the size and depth of subsurface voids (sinkholes) to treat loos of the irrigation water. The conducted GPR data were processed using the software program (Reflex W, 2D/3D). This program is designed for the steps of processing and interpretation of 2D and 3D electromagnetic and seismic reflections. The program supports most formats of the GPR data. As part of the standard filter algorithms, a wide range of special methods is available. The raw GPR data were processed using several parameters and filters to get clear high-resolution 2D GPR profiles (Sato, 2001).

Using ReflexW software, version 7.0 (Sandmeier 2012), the 2D data processing routine comprised:

IMPORT – involve file format conversion (*.dzt - output from SIR3000 equipment, to *.dat format - ReflexW file);

SET TIME ZERO - adjust of the first arrival of the electromagnetic wave;

ENERGY DECAY (gain) - applied to recover the attenuated amplitude of the electromagnetic signal during signal propagation;

BACKGROUND REMOVAL (2D filter) - remove coherent noise related to the reverberation of the electromagnetic wave within the antenna shield and external noises;

BANDPASS (1D filter) – eliminate of electronic and static noise inherent to the system;

LINEAR GAIN – applied to highlight the amplitudes lost with spherical scattering.

2.4. Data interpretation and analysis

GPR is a geophysical tool that produces vertical cross-sectional images of the shallow subsurface, similar to seismic reflection profiles. GPR data

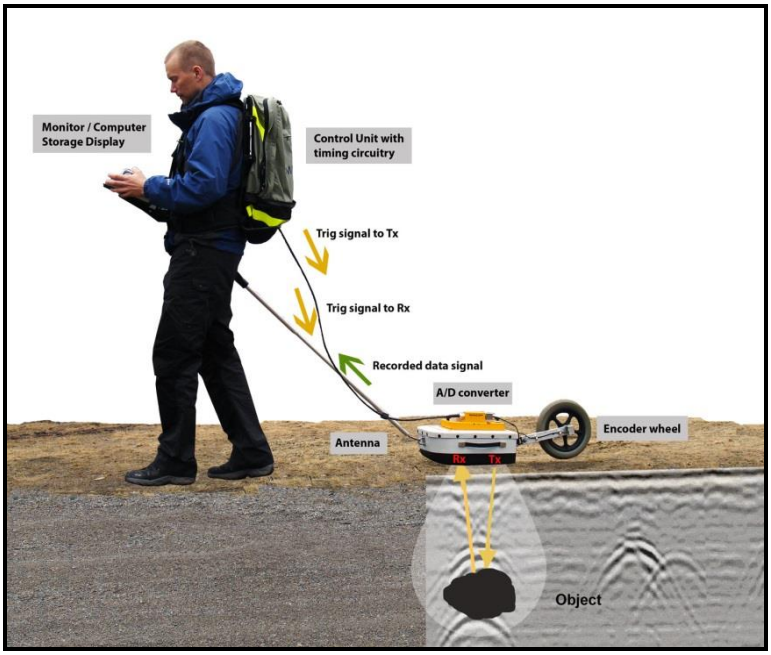

Fig. 3: The used GPR MALA System in the selected area.

collection provides the reflection and scattering of high-frequency electromagnetic waves within the subsurface (Gutierrez et al. 2009 and Mustasaar et al. 2012). If the subsurface layers were homogenous, the GPR instrument could not record any reflections. But earth crust is heterogeneous, and therefore gives radar reflection data to interpret (Hempen and Hatheway, 1992 and Daniels, 1996). The analysis of the reflected GPR signals is important because it gives notice of subsurface changes in lithology and other physical properties. The higher the contrast at a buried object, the greater the amplitude of the reflected waves. The amplitude changes can be related to the presence of important buried objects. The location of high and low reflectivity at specific depths can detect the possible buried objects with the surrounding soil. Areas of low amplitude reflections indicate uniform matrix materials or background soil, while those of high amplitude waves denote areas of high subsurface contrast, such as voids or gap features (Conyers and Goodman 1997). The gathered sixteen GPR profiles were divided into four groups to be processed and analyzed as follows:

A- Group 1 (P_1-P_4)

The length of each of these profiles is 34 m with a separation of one meter (Fig. 4). Observing the reflecting signals of the subsurface media provides information about the hidden layers of underground in these profiles.

In P_1 and P_2, the reflected signals are nearly similar, indicating the lock of possible hidden targets. The arrows in P_2 refer to the locations of possible slop cracks including wet soil, which gives high contrast color for the reflected signals. In P_3 and P_4, the black circles show signals scattering with a different contrast color than the surrounded soil, this indicates the possible gaps or voids as a collection of underground water coming through the slop cracks. The depths of the possible hidden voids are estimated to be about 7 and 8 m for P_2 and P_4 respectively.

B- Group 2 (P_5-P_8)

These profiles have different lengths that range between from 32and34 m with a separation of 1m (Fig. 5). The four GPR profiles include signals reflection, low, medium, and high reflection with a variation in the color contrast. The low and medium reflections refer to the soil bed layers and the high reflection indicates the possible hidden voids. The black arrows show possible slop cracks for passing underground water to possible subsurface voids indicated by the black circles. By visual inspection of the reflected signals inside these circles, reflections and scattering inside the circles are relatively higher than the surrounded soil, so the circles may indicate the presence of possible voids at these locations. The high contrast color of the reflected signals in these profiles may indicat to the wet parts of the soil. The possible hidden gaps or voids have depths of about 7m in P_5 and P_7 profiles and 8m in P_6 and P_8profiles.

C- Group 3 (P_9-P_{12})

This group includes four profiles P_9, P_{10}, P_{11}, and P_{12} (Fig. 6), with various lengths that range from 32to34 m with separation of one meters. Observing the reflected signals compare to the background reflections, there is no marked variation in the strength of these reflections and all are relatively similar in the color contrast except for some locations that have high pink colors. These locations indicate the wet soil and water-saturated parts of the subsurface soil, P_9 and P_{11}profiles. For these reasons, there are no clear voids in profiles, P_{10} and P_{12}.

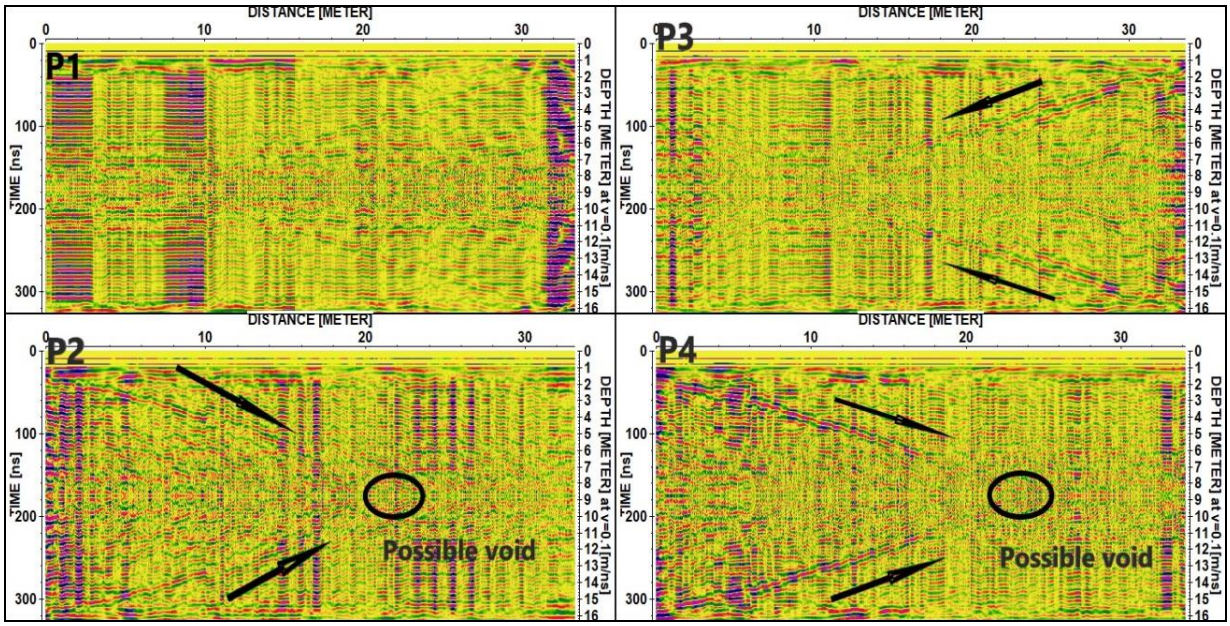

Fig. (4): GPR profiles P_1-P_4.

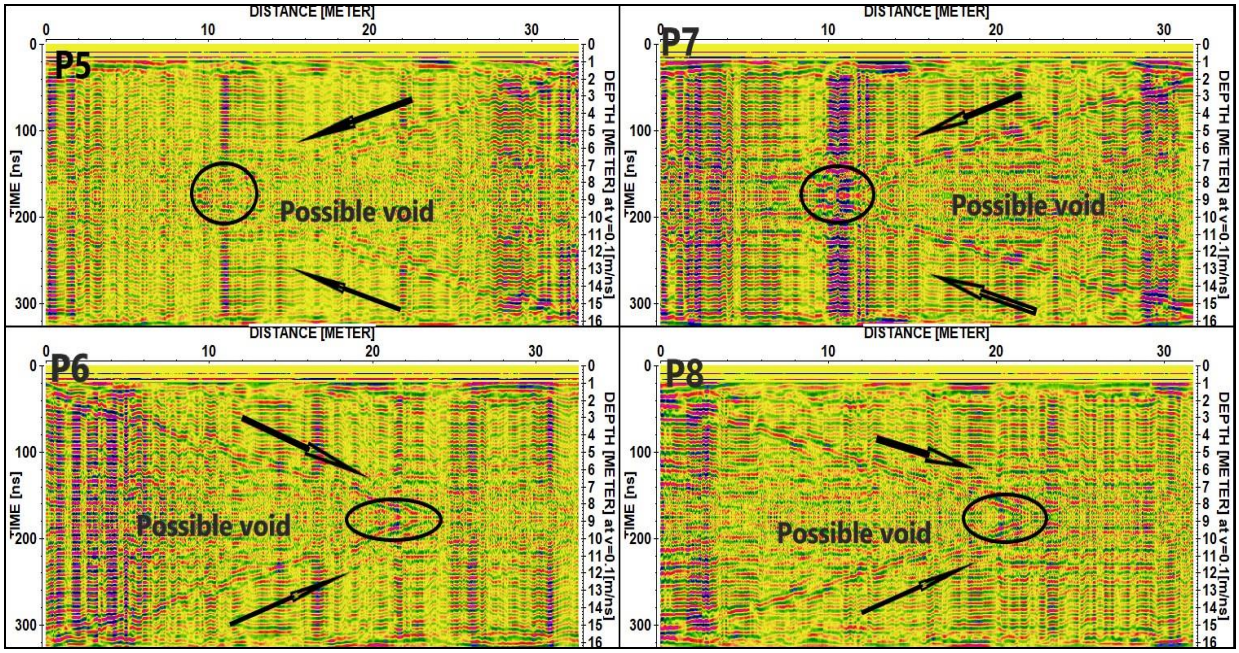

Fig. (5): GPR profiles P_5-P_8.

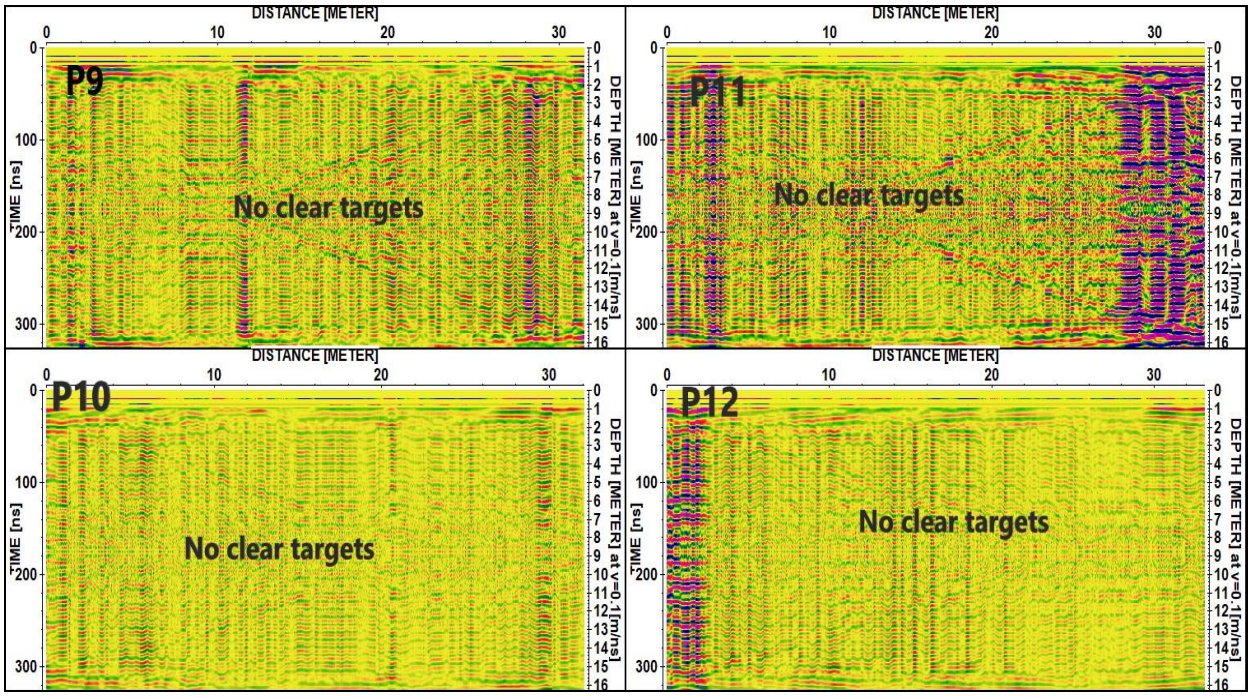

Fig. (6): GPR profiles P_9-P_{12}.

D- Group 4 (P_{13}-P_{16})

The length of the GPR profiles in this group is nearly similar (34m) with a separation of 1m (Fig. 7). Three Profiles (P_{13}, P_{14}, and P_{15}) have no high variation in reflection strength and the signals scattering, so the presence of any hidden voids observed and appear smooth, except for some parts of the soil with high contrast color indicating the wet and water-saturated parts Thus there are no clear evidence of possible hidden targets under these profiles. In the GPR profile (P_{16}), there is a relatively high reflection and scattering (indicated to by the black arrows and circle) for the signals with high contrast color compared to the surrounding soil. These features may indicate the locations of the possible slop cracks and void in this profile. The depth of the possible hidden void is about 7m.

3D Analysis

The GPR data were processed by different filters to improve the quality of the profiles for a perfect interpretation of the 2D radar images and delineating the depths of the hidden features. The results of the GPR data interpretation showed that the depths of these targets are 7m in profiles (P_2, P_5, P_7, and P_{16}) and were 8m in profiles (P_4, P_6, and P_{80}), equivalent to the TWTT of (140 - 190 ns). 3D analysis was performed on total GPR profiles to confirm the presence of the possible hidden features and estimates accurate depths of these objects. Four time-slicing at different TWTT were made (Fig. 8), two X-cut (10, 14 m. distance) and two Y-cut were performed at distances of 6 and 10 m (Fig. 9).

The time slices, X-cut and Y-cut confirm the presence of possible hidden target at TWTT ranges from 140 ns to 190 ns. These results are in agreement with the depth estimated from the 2D images, but the 3-D data analysis for the GPR data enabled better realization to the hidden features. The total information of the possible hidden voids (sinkholes) are gathered for presentation in Table 1.

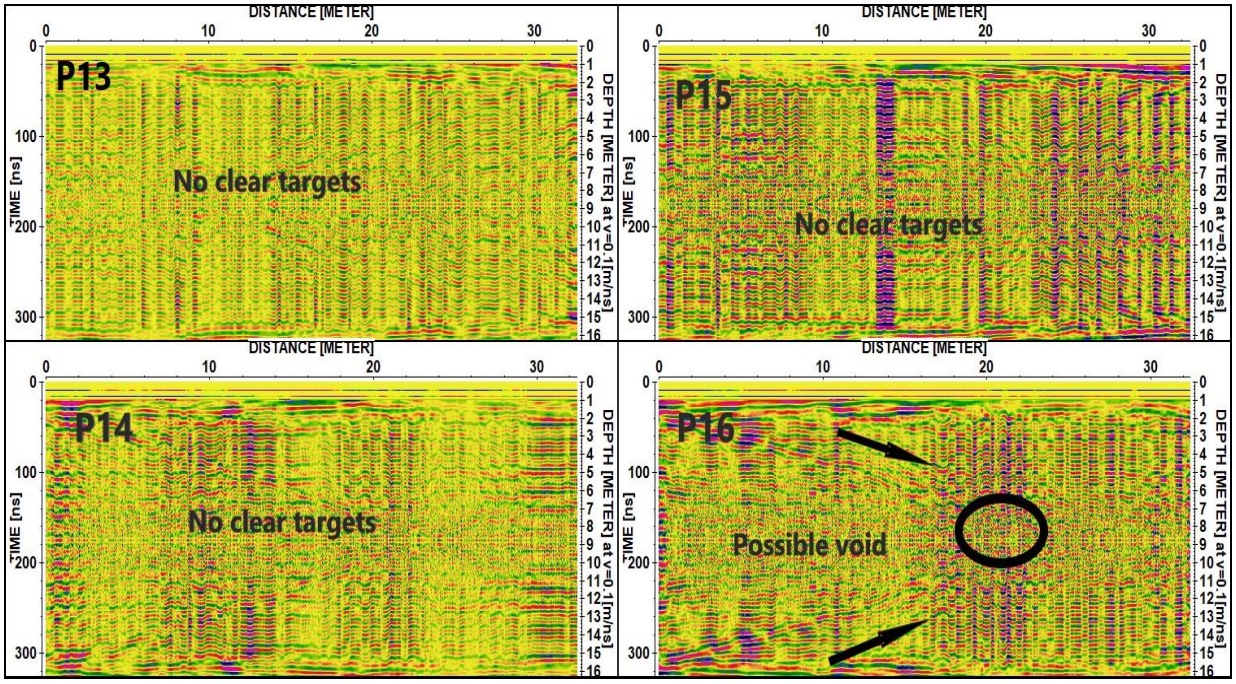

Fig. (7): GPR profiles P_{13}-P_{16}.

Table (1): The total information of the hidden possible voids (sinkholes) in the conducted GPR profiles of the study area.

Profile No.	Approximately TWTT	Approximately Depth	Approximately Size	shape
P2	140-190 ns	7m	2.5m	oval
P4	140-185 ns	8m	3m	oval
P5	140-180 ns	7m	3m	circular
P6	140-190 ns	7m	4m	oval
P7	140-180 ns	8m	3m	circular
P8	140-190 ns	8m	3.5m	oval
P16	140-190ns	7m	3m	Nearly circular

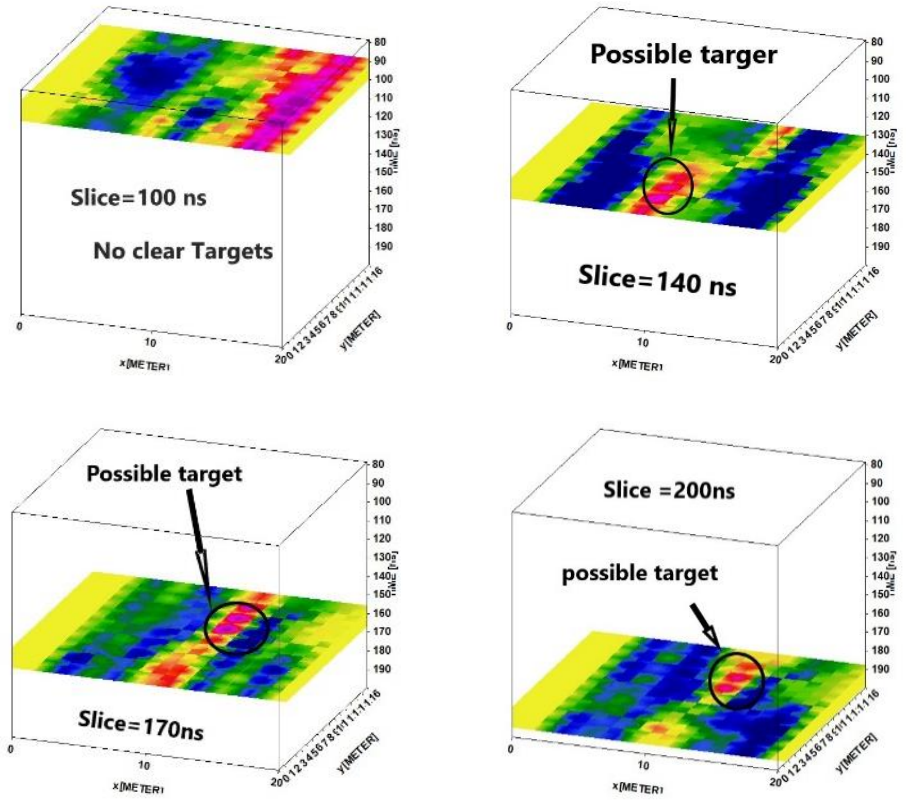

Fig. (8): 3D time slicing for the total GPR profiles.

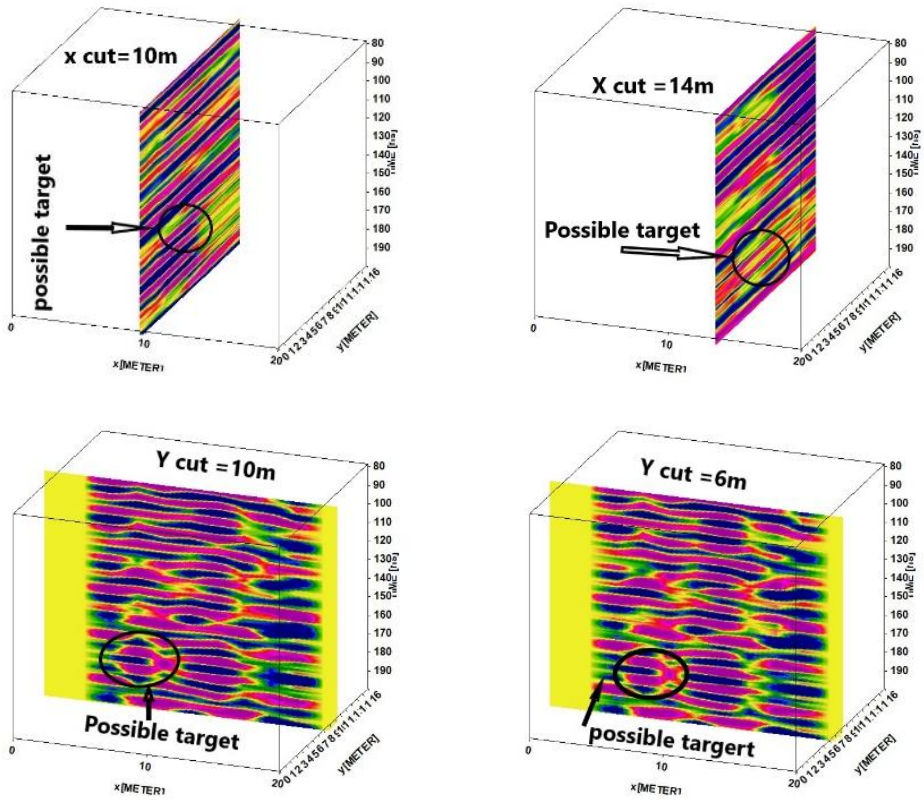

Fig. (9): 3D X-cut and Y-cut for the total GPR profiles.

CONCLUSIONS

The aim of the present study is to detect the subsurface voids or gaps (sinkholes) in the selected area to make up the loss of the irrigation water using the GPR technique. For this purpose, 16 GPR profiles were conducted of different lengths ranging from 32-35 m, with a line separation of 1 m. using the antenna of 100 MHz. The obtained GPR profiles were processed using the software program (Reflex W, 2D/3D) using different filters for achieving sound interpretation. The sixteen GPR profiles were divided into four groups, each one including four profiles.

The interpretation of GPR profiles from P_1 to P_{16}, reveals the locations of some possible voids or gaps (sinkholes), depending on the strength of wave reflections with its color contrast and amplitudes relative to the surrounding soil. These locations show different contrasts and high amplitudes of the reflected signals, compared to the surrounding soil. The scattering of the signals may be higher than the surrounded bed layers in these locations, which may reveal the presence of the possible voids or gaps in the study area.

The GPR data were processed in different ways to filter the profiles from noises to be interpreted accurately for the 2D radar images and to delineate the depths of the hidden possible targets. The results of the GPR data interpretation indicated that the depths of these targets were at 7m in profiles (P_2, P_5, P_7, and P_{16}) and at 8m in profiles (P_4, P_6, and P_8) which are equal to the TWTT of (140-190 ns). 3D analysis was performed for the total GPR profiles to confirm the presence of the possible hidden target and the accurate depths of these objects. Four time-slicing at different TWTT were made, also two X-cut at 10 and 14 m distance, and two Y-cut were done at distance 6 and10 m. The time slices, X-cut and Y-cut show the possible hidden target at TWTT ranges from (140- 190 ns). These results are in agreement with the depth obtained from the 2D image.

REFERENCES

Annan, A.P., 2002: GPR – History, Trends, and Future Developments. Subsurface Sensing Technologies and Applications. Vol. 3 (4): 253-270. https://doi.org/10.1023/A:1020657129590.

Bradford, J.H., 2007: Frequency-dependent attenuation analysis of ground-penetrating radar data. GEOPHYSICS, 72(3), J7–J16. https://doi:10.1190/1.2710183

Casas, A., Pinto, V., Rivero, L., 2000: Fundamental of ground penetrating radar in environmental and engineering applications. Ann. Geophys. 43 (6).

https://doi.org/10.4401/ag-3689

Chalikakis, K., Plagnes, V., Guerin, R., Valois, R., & Bosch, F.P., 2011: Contribution of geophysical methods to karst-system exploration: an overview. Hydrogeology Journal, 19(6), 1169–1180.

https://doi:10.1007/s10040-011-0746-x.

Conyers, Lawrence B. and Dean Goodman, 1997: Ground-penetrating Radar: An Introduction for Archaeologists. Alta Mira Press, Walnut Creek, California.

Daniels, D.J., 1996: Surface-penetrating radar, in, IEEF Radar, Sonar, Navigation and Avionics Series 6, E. D. R.

Davis, J.L., and Annan, A.P., 1989: Ground-penetrating radar for high-resolution mapping of soil and rock stratigraphy. Geophysical prospecting, v.3e7, P. 531-551.

Gutierrez, J.P., Galve, P., Lucha, J., Bonachea, L., Jorda, R., 2009: Investigation of a large collapse sinkhole affecting a multi-storey building by means of geophysics and the trenching technique (Zaragoza city, NE Spain) Environ Geol 58:1107–1122.

Hempen, G.l., and A.W., Hatheway, 1992: Geophysical methods for hazardous waste site characterization, special pub. No. 3: Assn. Eng. Geol.

Hoover, R.A., 2003: Geophysical Choices for Karst Investigations. Sinkholes and the Engineering Environmental Impacts of Karst. https://doi.org/10.1061/40698 (2003)48.

Hussain, Y., Uagoda, R., Borges, W.R., Nunes, J., Hamza, O., Condori, C., Aslam, K., Dou, J., Cárdenas-Soto, M., 2020: The potential use of methods to identify cavities, sinkholes and pathways for water infiltration: a case study from Mambaí, Brazil. Online in https://doi.org/10.1002/essoar.10503456.1

Kruse, S., Grasmueck, M., Weiss, M., Viggiano, D., 2006: Sinkhole structure imaging in covered Karst terrain. Geophysical Research Letters, 33(16).

https://doi:10.1029/2006gl026975 .

McMechan, G.A., Loucks, R.G., Zeng, X., Mescher, P., 1998: Ground penetrating radar imaging of a collapsed paleocave system in the Ellenburger dolomite, central Texas. Journal of Applied Geophysics, 39(1), 1–10.

https://doi:10.1016/s0926-9851 (98)00004-4

Motoyuki Sato, 2001: Jung-Ho Kim, RADPRO/GPR V.3.0 User's Guide.

Mustasaar, M., Plado, J. & Jõeleht, A., 2012: Determination of electromagnetic wave velocity in horizontally layered sedimentary target: a ground penetrating radar study from Silurian limestone, Estonia. Acta Geophysica, 60, 357–370

Rodriguez, V., Gutiérrez, F., Green, A.G., Carbonel, D., Horstmeyer, H., Schmelzbach, C., 2014: Characterizing Sagging and Collapse Sinkholes in a Mantled Karst by Means of Ground Penetrating Radar (GPR). Environmental & Engineering Geoscience, 20(2), 109–132.

https://doi:10.2113/gseegeosci.20.2.109.

Said, R., 1981: The geological evolution of the River Nile. Springer-Verlag, NewYork, 151P.

Sandmeier, K.J., 2012: REFLEXW Version 7.0 for Windows 9x/2000/NT/XP. Program for the processing of seismic, acoustic or electromagnetic reflection, refraction and transmission data. Manual do Software, 192p

Sevil, J., Gutiérrez, F., Zarroca, M., Desir, G., Carbonel, D., Guerrero, J., Linares, R., Roque, C., Fabregat, I. 2017: Sinkhole investigation in an urban area by trenching in combination with GPR, ERT and high precision leveling. Mantled evaporite karst of Zaragoza city, NE Spain. Engineering Geology, 231, 9–20.

https://doi:10.1016/j.enggeo.2017.10.009

Sharma, Prem V., 1997: Environmental and Engineering Geophysics. Cambridge university press. United Kingdam.

Zisman, E.D., Wightman, M.J., Taylor, C., 2005: The Effectiveness of GPR in Sinkhole Investigations. Sinkholes and the Engineering and Environmental Impacts of Karst. https://doi:10.1061/40796 (177) 65.